

See discussions, stats, and author profiles for this publication at: <https://www.researchgate.net/publication/231656944>

Effect of Dimers on the Temperature-Dependent Absorption Cross Section of Methyl Iodide

ARTICLE *in* THE JOURNAL OF PHYSICAL CHEMISTRY · JULY 1996

Impact Factor: 2.78 · DOI: 10.1021/jp960809r

CITATIONS

27

READS

18

3 AUTHORS, INCLUDING:



Gabriela C. G. Waschewsky

13 PUBLICATIONS 395 CITATIONS

SEE PROFILE



Veronica Vaida

University of Colorado at Boulder

105 PUBLICATIONS 2,907 CITATIONS

SEE PROFILE

Effect of Dimers on the Temperature-Dependent Absorption Cross Section of Methyl Iodide

Gabriela C. G. Waschewsky, Robert Horansky, and Veronica Vaida*

The Department of Chemistry and Biochemistry, The University of Colorado, Boulder, Colorado 80309

Received: March 15, 1996; In Final Form: April 26, 1996[®]

Due to the implication of iodine chemistry in stratospheric ozone depletion, an accurate atmospheric lifetime of methyl iodide has recently become of interest. To calculate this lifetime, a reliable temperature-dependent UV photodissociation cross section, in the region that overlaps with available solar light, is vital. Unfortunately, measurement of this cross section is complicated by the fact that, at typical laboratory pressures, methyl iodide readily forms dimers whose ultraviolet absorption differs from that of the monomer and that dimer formation is also temperature-dependent. We use a combination of theory and experiment to separate the changes in the absorption due to the temperature dependence of dimer formation from the narrowing of the absorption band that results from rotational and vibrational cooling of isolated methyl iodide molecules. Calculation of the predicted absorption cross section shows that the valence band absorption spectrum narrows only slightly upon cooling from 25 to -73 °C (200 K). Absorption spectra were also measured experimentally at a range of pressures from 0.1 to 2.4 Torr and a range of temperatures from -22 to 100 °C. The temperature-dependent cross section measured at 0.1 Torr agrees well with the calculated temperature dependence. The spectra at higher pressures show strong pressure as well as temperature dependence. This pressure dependence allowed us to constrain the temperature-dependent equilibrium constant for dimer formation.

Introduction

Light-driven reactions play an important part in the chemistry of the atmosphere, controlling the mixing ratios and lifetimes of photoreactive species. Methyl iodide is an example of a molecule whose atmospheric lifetime is determined by its photodissociation cross section: absorption in the near ultraviolet results in rapid dissociation to iodine atom and the methyl radical. One of these products, iodine, has recently been proposed as a sink for ozone in the lower stratosphere of the midlatitudes and tropics,¹ resulting in renewed interest in methyl iodide's photochemistry. Photodissociation of methyl iodide formed by marine algae² is a major source of iodine in the atmosphere, producing 1–2 Tg iodine per year.³ Methyl iodide's atmospheric lifetime determines how much methyl iodide is transported to the stratosphere and thus the stratospheric mixing ratio of iodine. On the basis of the room temperature absorption cross section measured by Cox,⁴ Solomon and co-workers have calculated a lifetime in the tropical troposphere of at least 2.5 days.¹ A more accurate lifetime calculation hinges upon redetermination of the absorption cross section at atmospherically relevant temperatures and pressures. Interest in stratospheric iodine chemistry has led to the recent attempts to measure a temperature-dependent absorption cross section of methyl iodide.⁵ The following paragraphs detail how laboratory measurements of methyl iodide's temperature-dependent cross section can be confounded by the existence of dimers in the sample. The experiments described in this paper were motivated by the question of how to measure a reliable "dimer-free" temperature-dependent cross section of methyl iodide.

The first feature in the methyl iodide ultraviolet absorption spectrum is a broad featureless band, centered at 260 nm, corresponding to a transition to the dissociative valence state, the "A" state. Photodissociation of methyl iodide in the atmosphere results from transition to this state, leading to prompt^{6,7} dissociation of the C–I bond. Of the five spin–orbit states energetically accessible in this region, two are optically

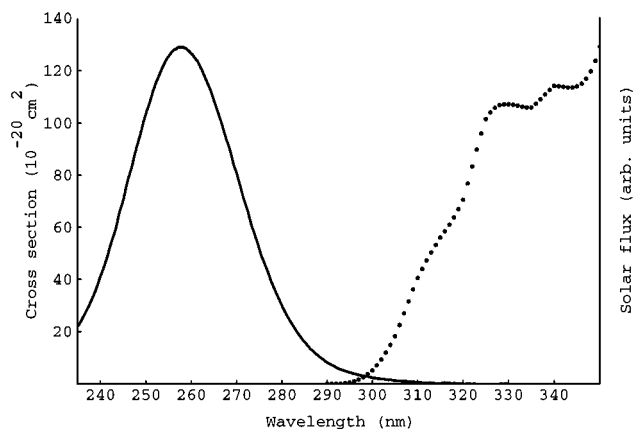


Figure 1. Room temperature absorption cross section of the A-band (valence) of methyl iodide, showing overlap with solar flux at sea level. The solar flux spectrum is adapted from data in ref 42. The methyl iodide spectrum was taken with a Cary 219 spectrometer at a resolution of 1.0 nm, with a period of 10 s, and a scan rate of 0.1 nm/s. The methyl iodide vapor was contained in a 12.6 cm jacketed cell with quartz windows, at a pressure of 300 mTorr at 298 K.

bright: a triplet state ($^3Q_0+$ in Mulliken's notation^{8,9}) that correlates diabatically to spin–orbit excited iodine ($^2P_{1/2}$) and ground state methyl, and a singlet state (1Q_1) which correlates to ground state iodine ($^2P_{3/2}$) and methyl. Most of the oscillator strength is in the transition to the triplet state, although the singlet state transition becomes more important at high energies.

The next feature in the UV absorption spectrum is a series of sharp peaks that correspond to a transition to a Rydberg state, the "B" state, with an origin at 201.2 nm. The Rydberg state is predissociated through surface crossings with the valence state.

Only the part of the valence band that overlaps with the sunlight filtered through stratospheric ozone ($\lambda > 290$ nm) is responsible for photodissociation in the atmosphere (see Figure 1). It has been suggested that the cross section in this low-energy tail would be especially sensitive to temperature.¹ The reason for this suggestion may be the assumption that absorption

[®] Abstract published in *Advance ACS Abstracts*, June 15, 1996.

by rotationally and vibrationally hot methyl iodide molecules contributes disproportionately to the low-energy edge of the absorption band, as is the case in acetylene^{10,11} and molecular iodine.^{12,13} We expect cooling of the molecules to narrow the spectrum, resulting in a reduction to the cross section of the low-energy tail. However, measurement of the temperature dependence of the methyl iodide absorption spectrum due to this rotational and vibrational cooling can be complicated by changes to the laboratory spectra due to the temperature dependence of dimer formation.

The photochemistry of methyl iodide clusters is well documented.^{14–23} Cluster formation causes a blue shift in the valence absorption band.¹⁴ The formation of the dimer is temperature-dependent: cooling increases the dimer population. The change in the low-energy tail of the absorption band that results from the temperature dependence of dimer formation can look very much like the expected decrease in the cross section due to rotational and vibrational cooling of the initial state. This effect of temperature-dependent dimer formation will appear in the laboratory spectra, yet the atmospheric mixing ratio of methyl iodide is too small for dimer formation to occur in the atmosphere.

In the Rydberg band, there is also a shift with dimerization, but the shift is to the red and very slight.¹⁴ The most obvious change in the Rydberg absorption band is the appearance of vibrational features that were absent in the monomer spectrum. The appearance of these features upon dimer formation offers a useful diagnostic tool for the detection of dimers in a sample.

Methyl iodide has been extensively studied as a test case for photoreaction dynamics of polyatomic molecules. A voluminous body of information, in both theory^{24–29} and experiment,^{6,7,30–38} is thus available to us. This lode of information includes calculated potential energy surfaces^{25–27} and experimental characterization of the photochemistry of methyl iodide clusters,^{14,15,17–23} both of which we draw from in the investigation that follows.

This study, a combined campaign of theory and experiment, separates the temperature and dimer effects on the absorption cross section of methyl iodide and discusses the methyl iodide spectra at temperatures relevant to the atmosphere. In the following sections we describe the procedure we used to measure methyl iodide absorption spectra in a range of temperatures and pressures, as well as our calculation aimed at predicting the temperature-dependent cross section of methyl iodide at atmospheric concentrations and temperatures. Finally, we compare the measured and calculated spectra, to provide a reliable prediction of the temperature dependence of methyl iodide's photodissociation cross section and thus its atmospheric lifetime. From the comparison of measured and calculated spectra, we were also able to constrain the value of the temperature-dependent equilibrium constant for the dimerization reaction.

Procedure and Data Analysis

Measurement of Absorption Cross Section of Methyl Iodide at a Range of Temperatures and Pressures. A Cary 219 spectrometer was used to measure methyl iodide ultraviolet absorption spectra at four different pressures, 2.4, 1, 0.3, and 0.1 torr, and six different temperatures, –22, 0, 25, 50, 75, and 96 °C. We measured A-band spectra, at all temperatures, from 290 to 335 nm, at 1 nm resolution, with a period of 10 s and a scan rate of 0.1 nm s^{–1}. A state spectra taken at 0.3 nm resolution showed no difference from those taken at 1 nm resolution. To follow the temperature dependence of the whole A-band, we also measured spectra from 235 to 290 nm at –22,

25, and 96 °C. B-band spectra were measured at all temperatures and pressures, from 196 to 203 nm, at 0.1 nm resolution, with a 10 s period and 0.01 nm s^{–1} scan rate.

To make up for the large difference in cross section between the A- and B-bands, a 12 cm cell was used for the A state measurements, while the B state spectra were taken in a 1 cm cell. Using two cells allowed us to take both spectra at the same pressure without saturating the stronger B-band, except at the highest pressures, or losing signal-to-noise in the spectrum of the much weaker A-band. The cells were jacketed to allow cooling or heating of the sample, and the quartz windows were doubled, with an evacuated layer between them, to prevent condensation onto the windows. The two cells were connected with copper tubing, so that the pressure and temperature of the gas in each cell would be the same. A special mount was designed so each cell could be moved into and out of the beam path, at each change in temperature, without losing alignment. Some error was introduced by the need to remove the cells from the mount at each change of pressure, but care was taken to minimize this error by aligning the cells in the mount to achieve the same absorption reading in all cases.

Ethylene glycol circulated through the jacket of each cell, through a Neslabs circulating constant temperature bath, cooled or heated the cells to the desired temperatures. We allowed 15 min equilibration time for each temperature. To test whether this time period would suffice, the ν_2 hot band 1251 cm^{–1} to the red of the B state origin was monitored at each temperature change in both cells.

We monitored the change in temperature of the sample via the Boltzmann population of the $\nu_2(\nu=1)$ level in the ground state. The integrated cross section of this hot band versus temperature was fit to the predicted Boltzmann distribution of the relative population of this vibrational level. Good agreement with the fit suggests that thermal equilibrium was achieved in all cases for the 12 cm cell and very likely also in the 1 cm cell, though the error here is larger, given the poor signal-to-noise.

Methyl iodide, from Aldrich, was degassed with three freeze–pump–thaw cycles before being delivered to the cells through a vacuum manifold. The pressure delivered to the cells, and the final pressure at the end of a run, was measured with a baratron capacitance manometer in the 10 Torr range.

The analog spectra, which were recorded on chart paper by the Cary 219, were digitized using an HP Colorpro plotter and a digitizing program and laser pen from Unplot-it. The highest possible resolution was used (0.002 in.), giving points spaced at about 0.025 nm for the A state spectra and 0.0025 nm for the B state spectra.

Before taking methyl iodide spectra, a background spectrum was measured for each cell, under the same conditions as the methyl iodide spectra. The background spectrum of the 12 cm cell was measured at 298 K from 235 to 335 nm, at a resolution of 1 nm; that for the 1 cm cell was measured at 298 K, from 196 to 210 nm, with a resolution of 0.1 nm. After background subtraction, the base line of each valence spectrum was adjusted to give zero absorbance at 335 nm. Scans that didn't extend to 335 nm were base-line-adjusted to match the scans (at the same pressure and temperature) that did.

To determine the number density at each nominal pressure, the maximum absorbance of the room temperature valence spectrum at that pressure was converted to $\epsilon = 336 \text{ L mol}^{-1} \text{ cm}^{-1}$ ³² using the relation

$$\log I_0/I = A = \epsilon cl = \epsilon(N/N_A)l \quad (1)$$

where N is number density, N_A is Avogadro's number, c is

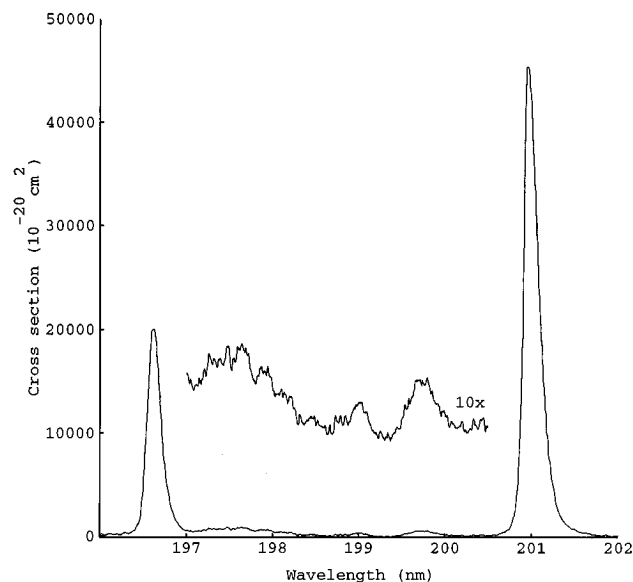


Figure 2. Room temperature absorption cross section of the B-band (Rydberg) of methyl iodide. The spectrum was measured using a Cary 219 spectrometer with 0.1 nm resolution, a period of 10 s, and a scan rate of 0.01 nm/s. The pressure in the 1 cm cell was 300 mTorr at 298 K.

concentration, and l is path length. A 1 nm breadth of points (approximately 40 points) at the maximum were averaged from two room temperature (298 K) scans at each pressure. Since each set of measurements started and ended at 298 K, these two scans usually bracketed the run. Thus, the given number density reflects the average number density over that set of measurements, which varied at most 3.5%.

We compared each number density determined from spectra with the pressure measured with the capacitance manometer and found good agreement (agreement varied from 0.5 to 5%).

Absorbance was converted to cross section, σ , for all spectra using the number densities determined as described above and the relation

$$\ln I_0/I = \sigma Nl \quad (2)$$

giving

$$A = 2.303\sigma Nl \quad (3)$$

Figures 1 and 2 show the absorption cross section, measured at 300 mTorr and 25 °C, of the valence and Rydberg states, respectively. The spectra compare well with the literature.^{30,32}

Calculation of Predicted Temperature-Dependent Cross Section. We used a simple reflection of the ground state wave functions onto the two optically bright A state potential energy surfaces to predict the temperature dependence of the isolated methyl iodide molecule. The method is depicted schematically in Figure 3.

Semiempirical excited state potential energy surfaces were calculated by Guo and Schatz.²⁵ The surfaces are based on a collinear model of methyl iodide dissociation. The three H atoms are replaced with a pseudoatom X. It is assumed that only two coordinates are important in the dissociation: the C–X distance r , and the distance R between I and the center of mass of CX. Bending and all rotational motions are ignored. Although only two degrees of freedom are used in their calculation, the curves are adjusted to reproduce an experimental spectrum³² using time-dependent wave-packet calculations.

The ground state potential energy surface is given by Shapiro.²⁷ Converting from Jacobian coordinates to dimension-

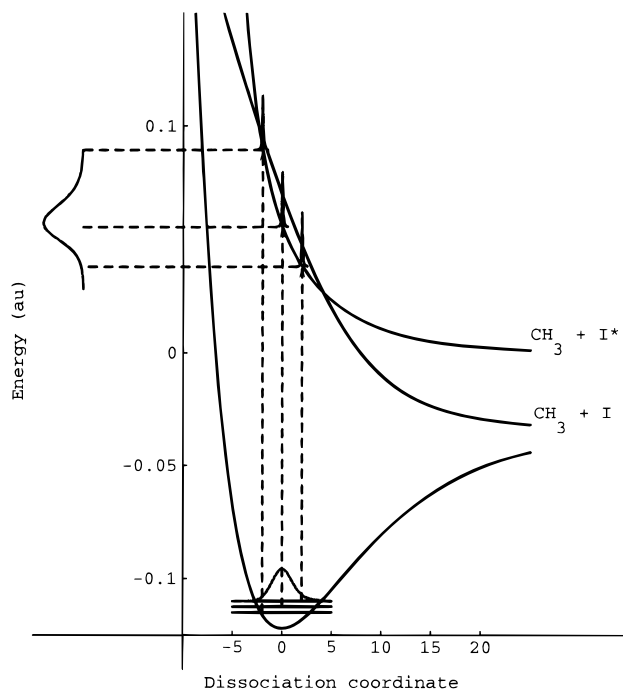


Figure 3. Cuts along the C–I dissociation coordinate, through the potential energy surfaces calculated semiempirically by Guo and Schatz (ref 25). The spectrum was calculated using a reflection technique. For a repulsive upper potential good results can be obtained by replacing the eigenfunction of the upper state by a δ function, centered at the classical turning point, as shown. The intensity of the transition is then proportional to $\nu\psi_{v'}^2$.

less normal coordinates (Q_1 , Q_2) was accomplished through relations worked out by Lee and Heller.²⁴

The zero-point energy is $GS(0,0) + \nu_1 + \nu_2$, where ν_i are the vibrations for Q_i . Using a harmonic oscillator approximation, $\nu_1 = 202 \text{ cm}^{-1}$, and $\nu_2 = 476 \text{ cm}^{-1}$. The initial ground state wave functions were approximated by the harmonic oscillator wave functions:

$$\psi(v=0) = \exp[-(1/2)Q_1^2 + (1/2)Q_2^2] \quad (4)$$

$$\psi(v=1) = Q_1Q_2 \exp[-(1/2)Q_1^2 + (1/2)Q_2^2] \quad (5)$$

The temperature-dependent rotational profile was determined from the rotational selection rules for the same linear triatomic described above and the Boltzmann relation for the population in the excited rotational levels. The population of the first vibrational state for the C–I stretch was similarly determined.

The energy of transition is the difference between the ground state zero-point energy + rotational energy and the excited state at a specific point on the coordinate system. From the Franck–Condon principle, the intensity of that transition is proportional to

$$\nu[\int \psi_{v'}\psi_{v''}]^2 \quad (6)$$

where $\psi_{v'}$ and $\psi_{v''}$ are the vibrational eigenfunctions of the upper and lower states. For a repulsive upper potential good results, and significant simplification of the above expression, can be obtained by replacing the eigenfunction of the upper state by a δ function, centered at the classical turning point, as shown in Figure 3. The intensity of the transition is then proportional to $\psi_{v''}^2$. The function, $\psi_{v''}^2$, is now simply “reflected” at the upper curve and multiplied by ν . Because the simple reflection method ignores the shape of the upper potential and its effect

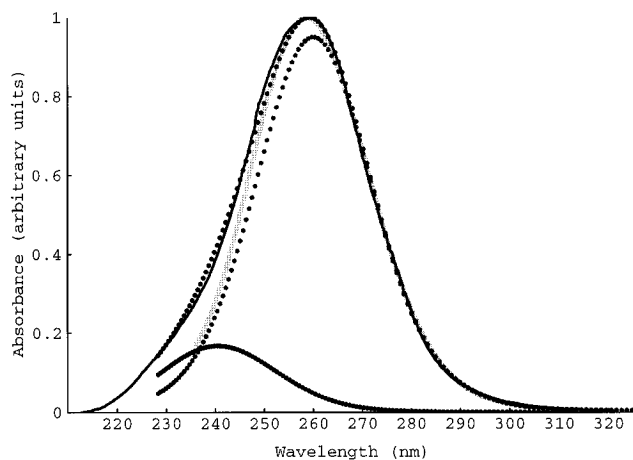


Figure 4. Comparison of calculated room temperature spectrum to our 300 mTorr room temperature spectrum and the spectrum calculated by Guo and Schatz (ref 25). Dotted lines are the calculated spectrum, showing contributions from transitions to the triplet and singlet states; the broad gray line is the measured spectrum shown in Figure 1, the thin line is the Guo and Schatz spectrum.

on the shape of the eigenfunction, a better fit to the measured spectrum was achieved by accounting for the slope of the upper potential.

The temperature dependence of the absorption comes from the Boltzmann population of rotational and vibrational states. Thus, the intensity of the transition from a particular rotation–vibration state must also be proportional to the population of that state.

Combining all these contributions, the intensity is proportional to

$$\left(\frac{\partial V}{\partial r}\right)^{-2} (2J'' + 1) e^{-\Delta E(J'', v'')/kT} \nu \psi_{v''}^2 \quad (7)$$

where $\partial V/\partial r$ is the slope of the upper potential surface and $\Delta E(J'', v'')$ is the energy of the ground electronic state rovibrational level from which the transition originates.

Rather than calculate an infinite number of points, each line in the spectrum is replaced by a Lorentzian function, with the final spectrum a sum of the Lorentzians. The number of lines (and thus the amount of computer time required for each calculation) versus the width of the Lorentzian was adjusted to give a smooth final spectrum without artificially broadening the spectrum, within a reasonable amount of computer time.

Spectra were calculated at three temperatures: 200, 298, and 373 K.

Figure 4 shows a comparison of our calculated room temperature spectrum with that calculated by Guo and Schatz, who describe the dissociation with a time-dependent quantum wave packet propagated using a fast Fourier transform method to solve the time-dependent Schrödinger equation. Since the surfaces were adjusted so that the spectrum would fit the experimental spectra of Gedanken and Rowe,³² the Guo–Schatz spectrum is also an accurate representation of the experimentally obtained spectrum of Gedanken and Rowe. Also shown is our spectrum measured at room temperature, at a pressure of 300 mTorr. The low-energy portion of the spectrum fits well with both theory and experiment. Figure 5c shows a close-up of the temperature-dependent cross section from 290 to 335 nm.

Discussion

Effect of Intermolecular Interactions on the Spectra of $(\text{CH}_3\text{I})_2$. Clusters can be used to study the effect of intermolecular interactions on the reactive processes of molecules in a

solvent or other complex environment. Dissociation dynamics are known to be strongly influenced by solvents. In addition to the solvent cage effect, which can inhibit dissociation either sterically or by collision-induced transfer of energy away from the excited molecule, dissociation can be influenced by electronic interaction between only a few molecules. In fact, interaction with only one perturbing molecule can produce a shift in the potential surfaces that influences the dissociation dynamics. This solvent-induced shift in the dissociative potential is the reason for the difference in the spectroscopy and reactivity of methyl iodide monomers and dimers.

Donaldson *et al.* have measured a 500–1000 cm^{-1} blue shift in the valence absorption band of methyl iodide upon cluster formation.¹⁴ They suggest that the shift is due to differential solvation of the ground state methyl iodide versus the valence state.^{14,15,19,23} Ground state dimers are stabilized by a dipole–dipole interaction. The valence transition involves the promotion of an electron from a nonbonding orbital on the iodine to an antibonding orbital centered on the C–I bond, so the excited state dipole is smaller than that in the ground state. The excited state dimer is therefore not as stabilized as the ground state dimer.

The spectral features of the Rydberg state, in contrast, show that it has a geometry and symmetry very much like the ground state.³³ It is not surprising, then, that the transition to the Rydberg state ($X \rightarrow B$) is hardly shifted at all, since the Rydberg state is as stabilized by dipole–dipole interaction as the ground state is. The most obvious change in the Rydberg spectrum, upon dimer formation, is the appearance of vibrational features not seen in the monomer spectrum. This change can be explained by assuming that dimerization causes a change in the predissociative curve crossing.¹⁶ Because of the difference in stabilization of the Rydberg and valence states, the result of dimer formation is a reduction in the Rydberg state energy versus that of the valence. The curve crossing is thus shifted to higher energy in the dimer. Because of the higher energy curve crossing, the “new” vibronic states dissociate more slowly. This longer lifetime leads to a narrowing of the line widths of these peaks, so transitions to these vibrational states now can be observed above the background. The Rydberg spectrum can therefore be a useful measure of the amount of dimers in a sample.

Separation of Temperature and Pressure Effects To Determine “Dimer-Free” Spectra at Atmospherically Relevant Temperatures. Armed with this understanding of the spectroscopy of methyl iodide monomers and dimers, we can predict the effect dimer contamination can have on the measured temperature-dependent absorption cross section. The spectral evidence implies that the ground state of the dimer is more stable than that of the monomer. Thus, as the temperature is lowered, the equilibrium constant for dimer formation becomes even more favorable:

$$K_p = \exp(-\Delta G^\circ/RT)$$

and the percentage of dimers increases. This increase in dimers in the cooled sample results in an increasing blue shift of the valence spectrum.

In the part of the spectrum that overlaps with available solar radiation, shown in Figure 1, this blue shift in the absorption is indistinguishable from the change in absorption expected from a narrowing of the absorption band due to cooling of vibrational and rotational levels in the ground state of isolated methyl iodide molecules. Only this rotational and vibrational cooling is relevant to a calculation of methyl iodide’s atmospheric photodissociation cross section. However, as we show in the

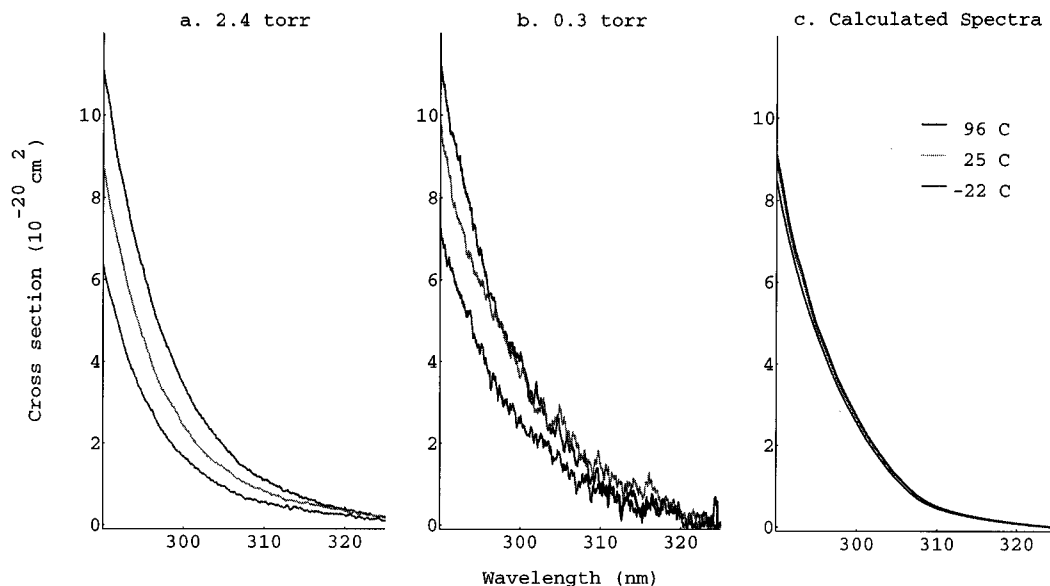


Figure 5. Temperature-dependent absorption cross section of the low-energy tail of the A-band of methyl iodide, shown at -22 , 25 , and 96 °C. (a) Temperature dependence of 2.4 Torr methyl iodide. (b) Temperature dependence at 300 mTorr. (c) Predicted temperature dependence of isolated methyl iodide molecules, at -73 , 25 , and 100 °C, based on the calculation described in the text.

following sections, the dimer contribution is manifest in most laboratory spectra and can have a significant effect on the measured temperature dependence.

The combined campaign of theory and experiment allowed us to separate these two contributions to the temperature dependence of the absorption, to obtain a dimer-free temperature-dependent absorption cross section for methyl iodide. We compared the temperature-dependent absorption cross section predicted by our calculation to temperature-dependent absorption cross sections measured at a range of pressures. The theoretical temperature dependence is equivalent to the zero-pressure limit and agrees with the temperature dependence we measure at the lowest pressure.

Figure 5 shows the temperature dependence of the absorption cross section from 290 to 320 nm at a high concentration and a low concentration, as well as the predicted temperature dependence based on our calculation. For each A state spectrum, the curves from 290 through 320 nm were integrated to give a temperature- and pressure-dependent cross section for the low-energy tail of the absorption band. Figure 6 shows the integrated absorbance versus temperature for each pressure.

The integrated absorbance, plotted versus temperature, clearly shows the pressure dependence, as well as temperature dependence, of the absorption. We know that when the absorbance is low enough to follow Beer's law, it is directly proportional to concentration (eq 3). Even at our highest concentration, the peak absorbance was only 13% of the maximum, within the limits of linearity; thus, if the temperature dependence were due entirely to monomer absorption, the slopes of these curves would be the same, though offset from each other due to the variation in concentration. The increase of the slope with increasing concentration is an indication of the amount of dimer in the sample.

Figure 6 also shows the predicted temperature dependence of isolated methyl iodide molecules, adjusted to same absorbance as the 0.1 Torr sample. It agrees well with the measured temperature dependence of this lowest pressure sample. It is also evident that even at the low temperatures encountered in the upper troposphere (200 K) the absorbance changes very little, suggesting that the temperature dependence of methyl iodide's absorption spectrum has a negligible effect on the calculation of its atmospheric lifetime.

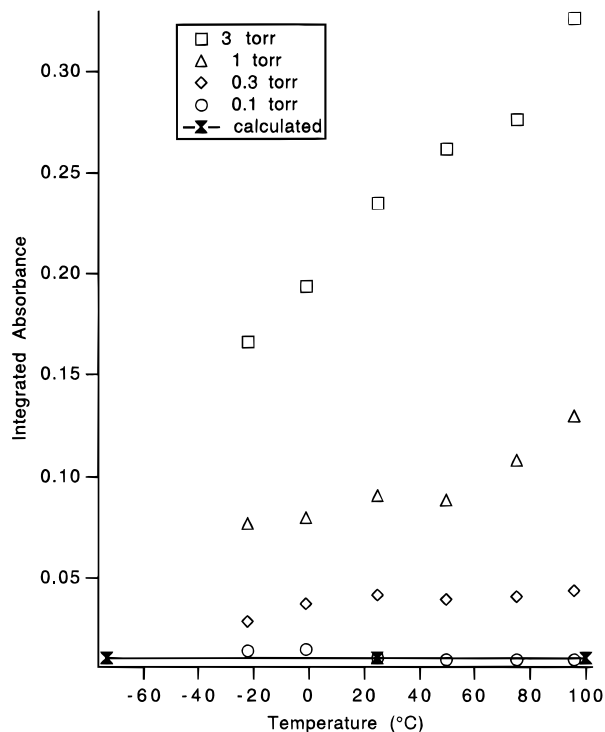


Figure 6. Integrated absorbance, over the region 290–320 nm, plotted versus temperature, clearly showing the pressure dependence, as well as temperature dependence, of the absorption.

Determination of Equilibrium Constant and Estimate of the Cluster Population. The pressure dependence of the temperature dependence allowed us to determine the dimer population present at each pressure and temperature. To do this, we made a few assumptions. First, knowing that the absorption band of the dimer is blue shifted relative to that of the monomer, we assumed that the dimer had negligible absorption in the region $\lambda \geq 290$ nm. Using the calculation described in the preceding section, we were able to predict the temperature-dependent cross section of the isolated methyl iodide monomer. This calculation predicts a temperature dependence much like that of our lowest pressure sample, as is evident in Figure 6. As the temperature is lowered, any decrease

in the integrated cross section, beyond that predicted by our calculation, we assume to be due to loss of the monomer population.

In the limit of negligible dimer population, the total pressure, $P_{T,0}$, is due to the monomer pressure, P_M . For each dimer produced, two monomers are lost; thus

$$P_M = P_{T,0} - 2P_D \quad (8)$$

The integrated cross section, C , is proportional to monomer pressure, and in the low-pressure limit of only monomers, C_0 is proportional to total pressure, so

$$C/C_0 = P_M/P_{T,0} = (P_{T,0} - 2P_D)/P_{T,0} = 1 - 2P_D/P_{T,0} \quad (9)$$

In addition, the dimer pressure is related to the total pressure, P_T , through the equilibrium constant, K .

$$K = P_D/(P_M)^2 = P_D/(P_T - P_D)^2 \quad (10)$$

We've already assumed a small dimer population, so that $P_D \ll P_T$; then,

$$K = P_D/(P_T)^2 \quad (11)$$

Substituting this relation for P_D into the above expression for C/C_0 , and equating P_T and $P_{T,0}$, gives

$$C/C_0 = 1 - 2KP_T \quad (12)$$

The values for C_0 were determined from the calculation described in an earlier section. The values for C were obtained by adjusting the integrated absorbance values shown in Figure 6 for the number density, N , at each pressure, through the relation shown in eq 3.

We performed a linear fit of C/C_0 versus pressure for each temperature, to obtain temperature-dependent estimates for K . The error in assuming P_D negligible became apparent at the lower temperatures, where the zero-pressure intercept deviated markedly from 1. At -22°C , a temperature for which the dimer population is far from negligible, the intercept was 0.85.

The equilibrium constant depends on temperature through its relationship to the Gibb's energy of reaction,

$$-RT \ln K_p = \Delta G^\circ = \Delta H^\circ - T\Delta S^\circ \quad (13)$$

Thus, a linear fit of $\ln K_p$ versus inverse temperature gives the enthalpy and entropy for the dimerization of methyl iodide, as shown in Figure 7.

$$\Delta H_{\text{dimer}} = -2.839 \pm 0.363 \text{ kcal mol}^{-1} = -993 \pm 127 \text{ cm}^{-1}$$

$$\Delta S_{\text{dimer}} = -2.6 \pm 1.2 \text{ cal mol}^{-1} \text{ K}^{-1}$$

On the basis of the blue shift of the dimer absorption relative to the monomer, Donaldson and co-workers¹⁴ estimated an enthalpy of dimerization of $500\text{--}1000 \text{ cm}^{-1}$. Although at the upper limit of this estimate, we are in agreement.

Taking the blue shift of 500 cm^{-1} as the lower limit for the dimer bond energy, and assuming an average frequency of 25 cm^{-1} for the six dimer-related vibrational modes, Donaldson and co-workers estimate a room temperature

$$-\Delta G = \Delta H - T\Delta S \approx 1430 \text{ cal mol}^{-1} - (298 \text{ K})(2.6 \text{ cal mol}^{-1} \text{ K}^{-1}) = 655 \text{ cal mol}^{-1}$$

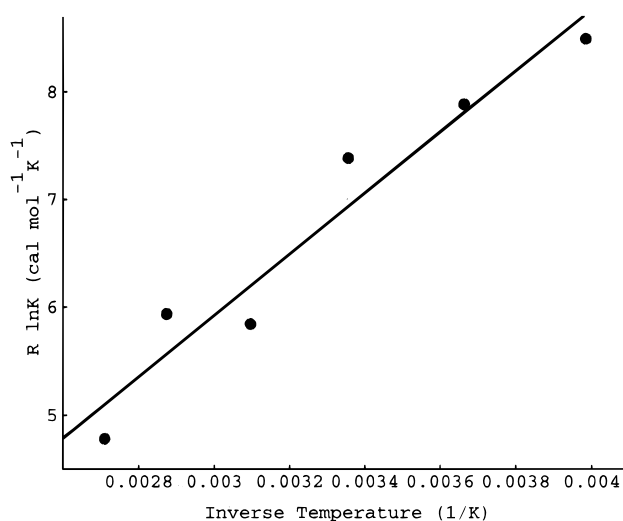


Figure 7. Temperature-dependent equilibrium constant for methyl iodide dimer formation reaction, determined from temperature and pressure dependence of methyl iodide absorption spectra, as described in the text.

TABLE 1: Dimer Proportion (%) in Typical Laboratory Samples^a

<i>P</i>	200 K <i>K</i> = 0.013–0.045	298 K <i>K</i> = 0.004–0.043	373 K <i>K</i> = 0.0008–0.016
0.1 Torr	0.1–4	0.04–0.4	0.0008–0.16
0.3 Torr	0.4–11	0.12–1.3	0.02–0.5
3.0 Torr	4–43	1.2–10	0.24–4.5
30.0 Torr	23–76	9.8–43	2.3–27
100.0 Torr	43–86	23–62	7–47

^a Percent dimer predicted using the temperature-dependent equilibrium constant (Torr^{-1}) determined from temperature and pressure dependence of absorption spectra, $R \ln K = 2839 \text{ cal mol}^{-1}/T - 2.6 \text{ cal mol}^{-1} \text{ K}^{-1}$, to give the higher values shown. The lower values are predicted using the equilibrium constant estimated by Donaldson and co-workers (ref 14), as described in the text.

to give the smaller equilibrium constants and dimer populations shown in Table 1. The table shows the percent dimers expected within the range of equilibrium constants constrained by Donaldson's estimate as a lower limit and ours as an upper limit.

Conclusion

Given the implication of methyl iodide photochemistry in the ozone depletion of the stratosphere^{1,39} and upper troposphere,^{4,40,41} we have analyzed the temperature dependence of the methyl iodide photodissociation cross section at laboratory and atmospheric pressures, to separate the dimer contribution to the temperature dependence from the temperature dependence of isolated methyl iodide monomers. Analysis of absorption spectra measured at a range of temperatures and pressures shows that the temperature effect at laboratory pressures results almost exclusively from the temperature dependence of dimer formation. The temperature dependence due to rotational and vibrational cooling of methyl iodide monomers is negligible in comparison.

The literature contains a number of calculated atmospheric lifetimes or J values for methyl iodide,^{1,3,5} based on room temperature^{2,4} or recently measured temperature-dependent spectra.⁵ But at most laboratory pressures, the measured temperature dependence is due to the temperature dependence of dimer formation and therefore is not an indication of the temperature-dependent absorption of the isolated molecule. As we have shown in the preceding sections, dimers contribute heavily to the temperature dependence of the absorption cross

section even at relatively low laboratory pressures. At these low pressures, the dimer concentration is small, as Table 1 shows. It is clear that even a small amount of dimers in a sample can measurably affect the temperature-dependent shape of the absorption spectrum. At higher pressures, the dimer effect can be overwhelming. On the other hand, the atmospheric mixing ratio of methyl iodide precludes dimer formation; thus, at atmospheric concentrations the only effect is that associated with the temperature-dependent Boltzmann population of excited rotational and vibrational levels in methyl iodide monomers. The calculated and low-pressure spectra both indicate that this temperature effect is slight. The atmospheric lifetime calculations based on this temperature-dependent absorption cross section should thus be virtually identical to earlier lifetimes^{1,3} calculated from the room temperature spectra.^{2,4}

Acknowledgment. The authors thank the NSF and the donors of the Petroleum Research Fund for financial support.

References and Notes

- (1) Solomon, S.; Garcia, R. R.; Ravishankara, A. R. *J. Geophys. Res.* **1994**, *99*, 20491–20499.
- (2) Chameides, W. L.; Davis, D. D. *J. Geophys. Res.* **1980**, *85*, 7383–7398.
- (3) Davis, D.; Crawford, J.; Liu, S.; McKeen, S.; Bandy, A.; Thornton, D.; Rowland, F.; Blake, D. *J. Geophys. Res.* **1996**, *101*, 2135–2147.
- (4) Jenkin, M. E. In *The Tropospheric Chemistry of Ozone in the Polar Regions*; Niki, H., Becker, K. H., Eds.; NATO ASI Series; Springer-Verlag: New York, 1993; Vol. 17.
- (5) Fahr, A.; Nayak, A. K.; Kurylo, M. J. *Chem. Phys.* **1995**, *197*, 195–203.
- (6) Dzvonik, M.; Yang, S.; Bersohn, R. *J. Chem. Phys.* **1974**, *61*, 4408.
- (7) Knee, J. L.; Khundkar, L. R.; Zewail, A. H. *J. Chem. Phys.* **1985**, *83*, 1996.
- (8) Mulliken, R. S. *Phys. Rev.* **1935**, *47*, 413.
- (9) Mulliken, R. S. *Phys. Rev.* **1936**, *51*, 310.
- (10) Ingold, C. K.; King, G. W. *J. Chem. Soc.* **1953**, 2702.
- (11) Innes, K. K. *J. Chem. Phys.* **1954**, *22*, 863–876.
- (12) Zare, R. N. *J. Chem. Phys.* **1964**, *40*, 1934–1944.
- (13) Steinfeld, J. I.; Zare, R. N.; Jones, L.; Lesk, M.; Klemperer, W. *J. Chem. Phys.* **1965**, *42*, 25–33.
- (14) Donaldson, D. J.; Vaida, V.; Naaman, R. *J. Chem. Phys.* **1987**, *87*, 2522–2530.
- (15) Donaldson, D. J.; Vaida, V.; Naaman, R. *J. Phys. Chem.* **1988**, *92*, 1204–1208.
- (16) Donaldson, D. J.; Child, M. S.; Vaida, V. *J. Chem. Phys.* **1988**, *88*, 7410–7417.
- (17) Fan, Y. B.; Randall, K. L.; Donaldson, D. J. *J. Chem. Phys.* **1993**, *98*, 4700–4706.
- (18) Momose, T.; Miki, M.; Uchida, M.; Shimizu, T.; Yoshizawa, I.; Shida, T. *J. Chem. Phys.* **1995**, *103*, 1400–1405.
- (19) Sapers, S. P.; Vaida, V. *J. Chem. Phys.* **1988**, *88*, 3638–3645.
- (20) Syage, J. A.; Steadman, J. *Chem. Phys. Lett.* **1990**, *166*, 159.
- (21) Syage, J. A. *Chem. Phys. Lett.* **1995**, *245*, 605–614.
- (22) Syage, J. A. *Chem. Phys.*, in press.
- (23) Vaida, V.; Donaldson, D. J.; Sapers, S. P.; Naaman, R.; Child, M. S. *J. Phys. Chem.* **1989**, *93*, 513.
- (24) Lee, S.-Y.; Heller, E. J. *J. Chem. Phys.* **1982**, *76*, 3035–3044.
- (25) Guo, H.; Schatz, G. C. *J. Chem. Phys.* **1990**, *93*, 393–402.
- (26) Amatatsu, Y.; Morokuma, K.; Yabushita, S. *J. Chem. Phys.* **1991**, *94*, 4858–4876.
- (27) Shapiro, M. *J. Phys. Chem.* **1986**, *90*, 3644–3653.
- (28) Shapiro, M. *J. Phys. Chem.* **1993**, *97*, 12473–12480.
- (29) Shapiro, M. *J. Phys. Chem.* **1993**, *97*, 7396–7411.
- (30) Baughcum, S. I.; Leone, S. R. *J. Chem. Phys.* **1980**, *72*, 6531.
- (31) Felps, S.; Hochman, P.; Brint, P.; McGlynn, S. P. *J. Mol. Spectrosc.* **1976**, *59*, 355.
- (32) Gedanken, A.; Rowe, M. D. *Chem. Phys. Lett.* **1975**, *34*, 39.
- (33) Guo, H.; Zewail, A. H. *Can. J. Chem.* **1994**, *72*, 947–957.
- (34) Hunter, T. F.; Lunt, S.; Kristjansson, K. S. *J. Chem. Soc., Faraday Trans. 2* **1983**, *79*, 303–316.
- (35) Lao, K. Q.; Person, M. D.; Xayariboun, P.; Butler, L. J. *J. Chem. Phys.* **1990**, *92*, 823–841.
- (36) Minchinton, A.; Cook, J. P. D.; Weigold, E.; von Niessen, W. *Chem. Phys.* **1985**, *93*, 21–38.
- (37) Scott, J. D.; Felps, W. S.; Findley, G. L.; McGlynn, S. P. *J. Chem. Phys.* **1978**, *68*, 4678–4687.
- (38) Strobel, A.; Fischer, I.; Lochschmidt, A.; Müller-Dethlefs, K.; Bondybey, V. E. *J. Phys. Chem.* **1994**, *98*, 2024–2032.
- (39) Solomon, S.; Burkholder, J. B.; Ravishankara, A. R. *J. Geophys. Res.* **1994**, *99*, 20929.
- (40) Jenkin, M. E.; Murrels, T. P.; Shalliker, S. J.; Hayman, G. D. *J. Chem. Soc., Faraday Trans.* **1993**, *89*, 433.
- (41) Wayne, R. P. *Chemistry of Atmospheres*; Clarendon Press: Oxford, 1991.
- (42) Finlayson-Pitts, B. J.; Pitts, J. N., Jr. *Atmospheric Chemistry: Fundamentals and Experimental Techniques*; Wiley-Interscience: New York, 1986; pp 121, 122.

JP960809R